Prefrontal cortex miR-874-3p prevents lipopolysaccharide-induced depression-like behavior through inhibition of indoleamine 2,3-dioxygenase 1 expression in mice

by Andi Jayalangkara

Submission date: 10-Mar-2022 04:31AM (UTC+0700)
Submission ID: 1780544223
File name: hibition_of_indoleamine_2,3-dioxygenase_1_expression_in_mice.pdf (1.92M)
Word count: 11735
Character count: 63452

Received: 26 May 2020 | Revised: 14 September 2020 | Accepted: 20 October 2020

DOI: 10.1111/jnc.15222

ORIGINAL ARTICLE

Journal of Neurochemistry JNC | WILEY

Prefrontal cortex miR-874-3p prevents lipopolysaccharide-induced depression-like behavior through inhibition of indoleamine 2,3-dioxygenase 1 expression in mice

Willy Jaya Suento[1,2] | Kazuo Kunisawa[3] | Bolati Wulaer[1,4] | Aika Kosuge[3] | Tsubasa Iida[3] | Suwako Fujigaki[1] | Hidetsugu Fujigaki[1] | Yasuko Yamamoto[1] | Andi Jayalangkara Tanra[2] | Kuniaki Saito[1,4,5] | Akihiro Mouri[3,5] | Toshitaka Nabeshima[4,5]

[1]Department of Disease Control and Prevention, Fujita Health University Graduate School of Health Science, Aichi, Japan

[2]Department of Psychiatry, Hasanuddin University Faculty of Medicine, South Sulawesi, Indonesia

[3]Department of Regulatory Science for Evaluation & Development of Pharmaceuticals & Devices, Fujita Health University Graduate School of Health Science, Aichi, Japan

[4]Advanced Diagnostic System Research Laboratory, Fujita Health University Graduate School of Health Science, Aichi, Japan

[5]Japanese Drug Organization of Appropriate Use and Research, Aichi, Japan

Correspondence
Akihiro Mouri, Department of Regulatory Science for Evaluation and Development of Pharmaceuticals and Devices, Fujita Health University, Graduate School of Health Sciences, Aichi, 470-1192, Japan.
Email: mouri@fujita-hu.ac.jp

Funding information
Japan Society for the Promotion of Science, Grant/Award Number: 17H04252, 17K01969, 18K15377, 18K19761 and 19K07490; Ministry of Education, Culture, Sports, Science and Technology of Japan (MEXT); Education and Research Facility of Animal Models for Human Diseases at the Fujita Health University

Abstract

Indoleamine 2,3-dioxygenase 1 (IDO1) is the first rate-limiting enzyme that metabolizes tryptophan to the kynurenine pathway. Its activity is highly inducible by pro-inflammatory cytokines and correlates with the severity of major depressive disorder (MDD). MicroRNAs (miRNAs) are involved in gene regulation and the development of neuropsychiatric disorders including MDD. However, the role of miRNAs in targeting IDO1 in the pathophysiology of MDD is still unknown. In this study, we investigated the role of novel miRNAs in the regulation of IDO1 activity and its effect on lipopolysaccharide (LPS)-induced depression-like behavior in mice. LPS up-regulated miR-874-3p concomitantly with increase in IDO1 expression in the prefrontal cortex (PFC), increase in immobility in the forced swimming test as depression-like behavior and decrease in locomotor activity as sickness behavior without motor dysfunction. The miR-874-3p increased in both neuron and microglia after LPS. Its mimic significantly suppressed LPS-induced IDO1 expression in the PFC. Infusion of IDO1 inhibitor (1-methyl-*l*-tryptophan) and miR-874-3p into PFC prevented an increase in immobility in the forced swimming test, but did not decrease in locomotor activity induced by LPS. These results suggest that miR-874-3p may play an important role in preventing the LPS-induced depression-like behavior through inhibition of IDO1 expression. This may also serve as a novel potential target molecule for the treatment of MDD.

KEYWORDS
depression, IDO1, lipopolysaccharide, miRNA-874-3p, prefrontal cortex

Abbreviations: 1-MT, 1-methyl-tryptophan; 3-HAA, 3-hydroxy anthranilic acid; 3-HK, 3-hydroxykynurenine; AA, anthranilic acid; CNS, central nervous system; FST, forced swimming test; HIP, hippocampus; IDO1, indoleamine 2,3-dioxygenase 1; IFN, interferon; IL, interleukin; KA, kynurenic acid; KYN, kynurenine; LPS, lipopolysaccharide; MDD, major depressive disorder; miRNA, microRNA; NC, miR-negative control; OFT, open-field test; PCNA, proliferating cell nuclear antigen; PFC, prefrontal cortex; QUIN, quinolinic acid; RRID, Research Resource Identifier (see scicrunch.org); TDO, tryptophan 2,3-dioxygenase; TLR4, toll-like receptor 4; TNF, tumor necrosis factor; TRP, tryptophan.

Willy Jaya Suento and Kazuo Kunisawa contributed equally to this work.

1 | Introduction

Major depressive disorder (MDD) is a complex mood disorder influenced by various genetic and environmental factors that affect 350 million people worldwide (Flint & Kendler, 2014). MDD is one of the leading causes of morbidity, mortality, and burden of health care utilization (Benton et al., 2007; Murray & Lopez, 1996; Otte et al., 2016). Although many studies have tried to optimize the treatment of MDD, about 40% of patients do not respond to the currently available treatments (Dwivedi, 2014; Fava & Davidson, 1996). This may be because of poor understanding of the pathophysiology of MDD.

It is well established that there is a strong correlation between inflammation and MDD. Multiple studies have shown that elevated levels of pro-inflammatory cytokines—such as tumor necrosis factor (TNF)-α, interleukin (IL)-6, and IL-1β—are found in the blood and postmortem brain of patients with MDD (Maes et al., 1997; Zou et al., 2018). Furthermore, interferon (IFN)-α therapy has been shown to induce depressive symptoms in patients with hepatitis C (Murakami et al., 2016).

Tryptophan (TRP) is an essential amino acid that acts as a precursor for the biosynthesis of the neurotransmitter serotonin (Badawy, 2017). Diminishment of the serotonin pathway has been proposed as a pathophysiological mechanism of MDD (Oxenkrug, 2013), although the majority of available TRP is metabolized through the kynurenine (KYN) pathway. Indoleamine-2,3-dioxygenase 1 (IDO1) is one of the two enzymes (the other is tryptophan 2,3-dioxygenase; TDO) metabolizing TRP through the KYN pathway. IDO1 is induced by several pro-inflammatory cytokines (e.g., TNF-α, IL-1β, and IFN-α) and lipopolysaccharide (LPS) (Fujigaki et al., 2017). Inflammatory conditions accelerate the KYN pathway, thus increasing the levels of neuroactive metabolites like 3-hydroxykynurenine (3-HK) and 3-hydroxy anthranilic acid (3-HAA) (Maes et al., 2011). These neuroactive metabolites play an important role in MDD pathophysiology (Dantzer et al., 2008; Fujigaki et al., 2017). Interestingly, increase in IDO1 activity has been positively correlated with scores for severe depression (Brad[illegible] et al., 2015). Reduced circulating TRP levels concomitant with increase in KYN metabolites have been reported in patients with MDD (Fujigaki et al., 2017; Savitz, 2017). In support of clinical studies, IDO1-mediated activation of the KYN pathway by systemic LPS injection results in both anxiety and depression-like behavior in mice (Salazar et al., 2012). More importantly, the IDO1 inhibitor, 1-methyl-*l*-tryptophan (1-MT), reverses LPS-induced depression-like behavior (Lawson et al., 2013; O'Connor, et al., 2009). These data strongly suggest that IDO1 may be a useful therapeutic target for MDD.

MiRNAs are short RNA molecules with an average of 22 nucleotides that are found in all eukaryotic cells (Bartel, 2004). They are post-transcriptional regulators that bind to complementary sequences on target mRNA transcripts, usually resulting in translational repression or gene silencing. They thus play an important role in the regulation of target mRNA expression (Cai et al., 2009; Schratt, 2009). MiRNAs are highly expressed in neurons and microglia of the central nervous system (CNS) and modulate both neuronal and immune functions (Brites & Fernandes, 2015). They are also involved in the development of neuropsychiatric disorders including MDD (Dwivedi, 2014; Karthikeyan et al., 2016; Mouillet-Richard et al., 2012; O'Connor et al., 2012). Recent preclinical studies have demonstrated that miRNA could have therapeutic potential for various CNS disorders, such as cognitive dysfunction (Tang et al., 2019) and MDD (Deng et al., 2019). However, it remains unclear whether the miRNAs inhibiting IDO1 is useful therapeutic targets for MDD.

In this study, we aimed to identify novel miRNAs that inhibit IDO1 activity and investigate whether it ameliorates LPS-induced depression-like behavior in mice.

2 | Materials and Methods

2.1 | Animals

Male C57BL/6J mice (8 weeks old; Research Resource Identifiers, RRID:IMSR_JAX:000664) were purchased from Japan SLC Inc. (n = 214). Only male mice were used to exclude any potential estrous cycle effects. This study was not pre-registered and no randomization/blinding was performed. No exclusion criteria were pre-determined, and no animals were excluded. Sample size for each experiment was determined based on our previous studies with the relevant type of experiment (Miwa et al., 2011; Mouri et al., 2018; Walker et al., 2020). No sample size calculations were performed. Mice were housed in a plastic cage and maintained on a 12-hr light/dark cycle (lights on at 8:00 a.m.) with food and water ad libitum. All experiments were carried out in accordance with the guidelines established by the Japanese Pharmacological Society and the Institute for Experimental Animals at Fujita Health University. The protocols were approved by the Ethics Committee of Animal Experiments at the Institute for Experimental Animals at Fujita Health University (Permit Number: AP16044).

2.2 | LPS injection

LPS (serotype E. coli 0127: B8, Cat# L3880; Sigma-Aldrich) was dissolved in phosphate-buffered saline (PBS). The mice were intraperitoneally (i.p.) injected with LPS (0.5 mg/kg) 24 hr before behavioral testing. This dose was used according to previous publication shown that LPS (0.5 mg/kg; i.p.) induced depression-like behavior in the forced swimming test (FST) (Yamawaki et al., 2018).

2.3 | Behavioral tests

All behavioral tests were performed between 10:00 a.m. and 6:00 p.m. To reduce the influence of the previous experiment, the

sequence of behavioral tests was arranged in order of stress level from low (open field test: Open-field test [OFT]) to high (forced swimming test: FST). The rotarod test was performed separate group of animals from the OFT and FST. Behavioral experiments were carried out in a sound-attenuated and air-regulated experimental room, to which the mice were habituated for more than 2 hr.

2.4 | Open-field test

OFT was performed as a previous report (Yamada et al., 2000) with minor modifications. The open field consisted of a square area with gray walls (42 × 42 × 40 cm) set in a dark, sound-attenuated room. The floor of the field was divided into nine identical squares with a light (200 lux) positioned 100 cm above the center of the floor. Each mouse was placed in one corner of the open field. The mice were allowed to explore the environment freely for 5 minutes. The time it took the mouse to move to another section was reported as its starting latency. The time spent in the center or other zone and the total distance traveled were measured using an ANY-maze video tracking system (Cat# 6000, Stoelting Co., Ltd.; RRID:SCR_014289). The number of rearing events was also counted by images captured on video.

2.5 | Forced swimming test

The FST was performed according to the method outlined in previous report (Murai et al., 2007). Each mouse was placed in a transparent glass cylinder (20 × 15 cm) that was filled with water to a depth of 13 cm, at a temperature of 22 °C, and illuminated by a lamp placed above the apparatus (100 lux). The mouse was forced to swim for 6 minutes. The duration of swimming was measured using SCANET-40 (Cat# MV-40, MELQUEST Co., Ltd.). The immobility time was calculated in the last 5 min as follows: Immobility time (s) = total time − swimming time.

2.6 | Rotarod test

The rotarod test was performed according to the method outlined in previous report (Iida et al., 1999) with minor modifications. Motor functions of the mice were examined using the rotarod test (Cat# 47650; Muromachi Kikai Co., Ltd.). The test was performed by placing a mouse on a rotating treadmill drum (3 cm diameter) with constant illumination of approximately 20 lux, and measuring how long the mouse was able to maintain its balance on the treadmill. Four trials were conducted in which the treadmill rotated at 12 rpm for a maximum of 120 seconds. Each mouse's mean latency to fall was calculated and used in subsequent analysis. To prevent experimental bias, a blinded observer calculated the latency.

2.7 | Sample collection

The mice were deeply anesthetized with isoflurane (1 ml/ml; Cat# 095-06573; Wako Pure Chemical Co.) and transcardially perfused with ice-cold PBS at 2, 6, 12, and 24 hr after LPS injection. The entire brain was quickly removed and chilled in ice-cold saline. The prefrontal cortex (PFC) and hippocampus (HIP) were manually dissected on ice-cold plates and then immediately frozen using dry ice because these regions have been associated with the pathophysiology and progression of MDD (McKinnon et al., 2009; Treadway et al., 2015). Specifically, the enhanced inflammation, oxidative stress, and neurotransmitter disturbances (e.g., serotonin, glutamate, gamma-aminobutyric acid) in PFC and HIP facilitate the MDD progression and contribute to further brain structural decline as the disease advances (Holmes et al., 2018; Setiawan et al., 2015). All samples were stored at −80°C until needed for analysis.

2.8 | Quantitative real-time reverse transcription PCR (qRT-PCR)

Total RNA was isolated using a NucleoSpin® RNA kit (Cat# U0955; Takara) according to the manufacturer's instructions. All qPCR primers were purchased from Integrated DNA Technologies. First-strand cDNA was synthesized using the ReverTra Ace qPCR RT kit (Cat# FSQ-101; Toyobo). For quantitative PCR, SsoAdvanced™ Universal Probes Supermix (Cat# 1725281; Bio-Rad) was used and subjected to real-time PCR quantification using a StepOne™ Real-Time PCR System (Cat# 4376357; Life Technologies). Quantitative PCR analysis was performed using a StepOne analyzer (Cat# 4461357; Life Technologies; RRID:SCR_014281). The PCR reaction program consisted of 40 cycles of 95°C for 30 seconds and 60°C for 1 minute. To discriminate specific amplification from non-specific amplification, a melting curve analysis was performed after each PCR reaction. β-actin was used as a housekeeping gene to normalize all PCR data.

Quantitative PCR for miRNA was isolated using a NucleoSpin® miRNA kit (Cat# U0971; Takara). All PCR primers were purchased from Applied Biological Materials Inc.. First-strand cDNA was synthesized using an miRNA cDNA synthesis kit (Applied Biological Materials Inc.). For the quantitative PCR, SsoAdvanced™ Universal SYBR® Green Supermix (Cat# 1725271; Bio-Rad) was used and then subjected to real-time PCR quantification using a StepOne™ Real-Time PCR System (Life Technologies). The PCR cycle was as follows: 95°C for 10 min, 40 cycles of 95°C for 15 seconds, and 60°C for 1 minute. A melting curve analysis was performed at the end of each experiment to verify that a single product per primer pair was amplified. U6 small nuclear RNA (U6 snRNA) was used as a housekeeping gene to normalize all PCR data.

Primers used in this study include: IDO1 (Mm.PT.58.2954917), IL-1β (Mm.PT.58.41616450), IL-6 (Mm.PT.58.10005566), TNF-α (Mm.PT.58.12575861), β-actin (Mm.PT.39.a.22214843), Mmu-miR-

203-3p (MPM00983), Mmu-miR-384-3p (MPM00461), Mmu-miR-874-3p (MPM02237), Mmu-miR-381-3p (MPM01286), U6 snRNA (MPM00002), and Universal 3′ miRNA reverse primer (MPH00000). Representative RT-PCR product bands are shown in Figure S1.

2.9 | Western blotting analysis

Western blotting was performed as described previously (Kunisawa et al., 2017). Tissues were homogenized in an ice-cold homogenization buffer (pH 7.4; 50 mM Tris-HCl [pH 8.0] containing 4 mM EGTA, 10 mM EDTA, 150 mM sodium dihydrogen phosphate, and 1% protease inhibitor cocktail) (Cat# 162-26031; Fujifilm Wako Pure Chemical Co.) by sonication. After 15 minutes of centrifugation at 15,300 *g* at 4°C, the protein concentration in the supernatant was determined with Quick Start™ Bradford 1x dye reagent (Cat# 5000205; Bio-Rad) and normalized to 2.0 μg/μL. Respective protein samples were then electrophoresed on 10% (w/v) SDS-PAGE and subsequently transferred onto a 0.22 mm PVDF membrane (Cat# GVWP04700; Millipore). The membranes were blocked with 5% skim milk in TBST for 60 minutes at room temperature (24°C) and probed with a primary antibody at 4°C overnight. Next, PVDF membranes were washed in TBST (three times for 10 minutes) and incubated in the appropriate HRP-conjugated secondary antibody for 2 hr at room temperature. The PVDF membranes were then washed again in TBST (3 times for 10 minutes) and reacted with Immobilon Forte Western HRP substrate (Cat# WBLUF0100; Millipore). Immunoreactive bands were visualized using ATTO LuminoGraphI (Cat# WSE-6100; ATTO). The band intensities were analyzed using ImageJ software. The primary antibodies used were rat anti-IDO1 (1:500; Cat# 53978; Santa Cruz Biotechnology; RRID:AB_831071), mouse anti-β-actin (1:1000; Cat# A5441; Sigma-Aldrich, RRID:AB_476744), and mouse anti-TLR4 (1:1000; Cat# sc-293072; Santa Cruz Biotechnology; RRID:AB_10611320). The secondary antibodies were diluted at 1:2000 for horseradish peroxidase-linked anti-rat or anti-mouse IgG (Cat# NA935 and NA931; GE Healthcare, RRID:AB_772207 and AB_772210).

2.10 | Mouse tissue preparation

For histological analysis, mice were deeply anesthetized with isoflurane (1 ml/ml, Wako Pure Chemical Co.). Once reflex responses had disappeared, mice were transcardially perfused with 4% paraformaldehyde in phosphate-buffered saline (PBS). Brains were post-fixed in 4% paraformaldehyde overnight at 4°C. The post-fixed tissues were cryoprotected overnight in PBS containing 20% sucrose, embedded in OCT compound (Cat# 45833; Sakura Finetechnical Co.), and cut into 20 μm sections using a cryostat (Cat# Leica CM3050, RRID:SCR_016844) for *in situ* hybridization and immunohistochemistry.

2.11 | *In situ* hybridization

Digoxigenin (DIG)-labeled single-stranded riboprobes for miR-874-3p were purchased from QIAGEN (Cat# YD00616271-BCG). The protocol for *in situ* hybridization was previously described (Kunisawa et al., 2018). Briefly, the 20 μm sections were treated with proteinase K (40 μg/ml for 30 min at room temperature; Cat# 107393; Millipore) and hybridized overnight at 50°C with DIG-labeled antisense riboprobes in a hybridization solution consisting of 40% formamide, 20 mM Tris-HCl (pH 7.5), 600 mM NaCl, 1 mM EDTA, 10% dextran sulfate, 200 μg/mL yeast tRNA, 1x Denhardt's solution, and 0.25% SDS. The sections were washed three times in 1× SSC (150 mM NaCl and 15 mM sodium citrate) containing 50% formamide at 50°C, followed by 0.1 M maleic buffer (pH 7.5) containing 0.1% Tween 20 and 0.15 M NaCl. The bound DIG-labeled probe was detected by overnight incubation with anti-DIG antibody conjugated with alkaline phosphatase (Cat# 11093274910; Roche). The probe was developed in a solution containing 4-nitro-blue tetrazolium chloride (NBT; Cat# 11383213001; Roche) and 5-bromo-4-chloro-3-indolyl phosphate (BCIP; Cat# 11383221001; Roche) in the dark at room temperature.

2.12 | Immunohistochemistry

Immunofluorescence staining was performed as described previously (Kunisawa et al., 2018). Cryosections were immunostained with a mouse anti-IDO1 antibody (1:500; Cat# MABF850; Millipore), mouse anti-PCNA antibody (1:1000; Cat# MS-106-P; Thermo; RRID:AB_64275), mouse anti-GFAP antibody (1:1000; Cat# SAB5201104; Sigma-Aldrich; RRID:AB_2827276), rabbit anti-NeuN antibody (1:1000; Cat# ab177487; Abcam; RRID: AB_2532109), rabbit anti-Iba1 antibody (1:500; Cat# 019-19741; Wako Pure Chemical Co.; RRID:AB_839504), and rat anti-F4/80 antibody (1:500; Cat# ab6640; Abcam; RRID:AB_1140040). The coronal sections between 1.42 and 2.10 mm from bregma (Paxinos & Franklin, 2004) were heated in a microwave in 10 mM citrate buffer (pH 6.0) up to 90°C for 5 minutes. After washing with PBS containing 0.3% Triton-X (PBST), sections were blocked with 5% fetal bovine serum (Cat# 174012, Nichirei Biscience Inc.) in PBST for 2 hr and then incubated with primary antibodies in PBST at 4°C overnight. After washing with PBST, the sections were incubated with secondary antibodies (1:2000; Alexa488-conjugated goat anti-mouse IgG and Alexa568-conjugated goat anti-rabbit IgG; Cat# A28175 and A11011; Molecular Probes; RRID:AB_2536161 and AB_143157) and Hoechst 33342 (0.1 μg/ml; Cat# 346-07951; Dojindo; RRID:KU039) for 3 hr at room temperature. Sections were then rinsed with PBST, mounted and covered with glass coverslips, and then visualized under a Zeiss LSM-710FSX100 confocal laser microscope (Olympus; RRID:SCR_018063). The immunohistochemical controls were performed as described above except for the omission of the primary antibodies. No positive immunostained cells were found in any of the controls.

Sections used for 3,3'-diaminobenzidine (DAB) staining were blocked with 5% fetal bovine serum (Cat# 174012; Nichirei Biscience Inc.) in PBST for 1 hr, then incubated with mouse anti-NeuN antibody (1:1000; Cat# ab177487; Millipore; RRID:AB_2532109) and rabbit anti-Iba1 antibody (1:500; Cat# 019-19741; Wako Pure Chemical Co., RRID:AB_839504) at 4°C overnight. After washing with PBST, the sections were incubated with secondary antibodies (1:400; biotinylated goat anti-mouse IgG and biotinylated goat anti-rabbit IgG; Cat# RPN1001 and RPN1004, Vector Laboratories, RRID:AB_1062579 and AB_1062582) for 1 hr at room temperature. The sections were then incubated with avidin-biotin complex (ABC) solution (horseradish peroxidase-streptavidin-biotin complex, Vectastain ABC kit; Cat# PK-6100; Vector Laboratories) for 1 hr at room temperature. The HRP signals were detected by DAB solution with 0.03% H_2O_2.

The number and density of cells positive for immunoreactivities were analyzed using ImageJ software. The average of at least three slices in each mouse was calculated in a 360 μm × 260 μm prelimbic area of the PFC and used for statistical analysis.

2.13 | Surgery and intracranial injections

The surgery was performed as described previously (Mouri et al., 2012). An miR-negative control (miR-NC; Cat# A07001) and miR-874-3p mimic (Cat# A03001) were purchased from GenePharma co. Mice were anesthetized with a mixture of anesthetic, muscle relaxant, analgesic and sedative such as medetomidine (0.3 mg/kg; Domitor®; Nippon Zenyaku Kogyo), butorphanol (5.0 mg/kg; Vetorphale®; Meiji Seika Pharma), and midazolam (4.0 mg/kg; Midazolam Sandoz®; Sandoz) to minimize the pain and reversed by atipamezole (0.15 mg/kg; Antisedan®; Nippon Zenyaku Kogyo) after completed the surgery. Stainless steel guide cannulas (9.7 mm, 0.4 mm inner diameter, 0.5 mm outer diameter; Cat# AG-6; Eicom) were bilaterally implanted into the PFC. The coordinates were +1.7 mm anterior and ± 0.5 mm lateral from the bregma, at a depth of 1.5 mm from the skull. The guide cannulas were fixed using dental cement (Cat# 204310196; Shofu Inc.). To seal the top of the guide cannula and prevent tissue entry into the cannula, a dummy cannula (0.3 mm in diameter; Cat# AD-6; Eicom) was left in place throughout the experiment. Three days after recovery from surgery, mice were injected with sterile endotoxin-free PBS (0.5 μl/site) or 1-methyl-l-tryptophan (1-MT: 1 μg/μL, 0.5 μl/site; Cat# 447439; Sigma-Aldrich) for 1-MT experiment, and miR-NC (100 nM, 0.5 μL/site), or miR-874-3p mimic (100 nM, 0.5 μL/site) for miR-mimic experiment bilaterally using a 27-gauge infusion needle (1.0 mm longer than the guide cannulas; Cat# 80300; Plastics One) connected to a 10 μl Hamilton microsyringe at a rate of 0.1 μl/min. After the injection, the needle was left in place for an additional 3 min before withdrawal. It is known that miRNA mimics have high stability *in vivo* and can be applied for microinjection (Krutzfeldt et al., 2005; Rupaimoole & Slack, 2017). The OFT and FST were performed 24 hr after the infusion.

2.14 | Measurement of KYN metabolites

The KYN metabolites were measured as described previously (Tashiro et al., 2017). For TRP, KYN, kynurenic acid (KA), anthranilic acid (AA), and 3-HAA, the PFC was weighed and homogenized (1:3, w/v) in 10% perchloric acid (Cat# 162-00715; Fujifilm Wako Pure Chemical Co.). After mixing, the precipitated proteins were removed by centrifugation (13,000 rpm, 15 min). Fifty microliters of the resulting supernatant were subjected to high-performance liquid chromatography (HPLC; Cat# SPD-M30A; SHIMADZU) analysis. TRP, KYN, KA, AA, and 3-HAA were isocratically eluted from a reverse phase column (TSKgel ODS-100V, 3 μm, 4.6 mm (ID) × 15 cm (L); Cat# 0021829; Tosoh Co.) using a mobile phase containing 10 mM sodium acetate and 2% acetonitrile (pH adjusted to 4.5 with acetic acid) at a flow rate of 0.8 mL/min. TRP and KYN were detected by ultra-violet and spectrophotometric apparatus (TRP [UV wavelength, 280 nm], KYN (UV wavelength, 365 nm); Cat# SPD-M30A; SHIMADZU). AA, 3-HAA, and KA were detected by a fluorescent detector (AA and 3-HAA [excitation wavelength: 320 nm, emission wavelength: 420 nm], KA [excitation wavelength: 344 nm, emission wavelength: 404 nm]; Cat# RF-20A; SHIMADZU).

For 3-HK, the PFC was weighed and homogenized (1:3, w/v) in 10% perchloric acid (Fujifilm Wako Pure Chemical Co.). After mixing, the precipitated proteins were removed by centrifugation (13,000 rpm, 15 min). Twenty microliters of the resulting supernatant was applied to a C18 octadecylsilyl (ODS) silica-gel column (2.1 mm × 150 mm; Cat# SC-50DS; Eicom) using a mobile phase consisting of 5% acetonitrile, 0.9% trimethylamine, 0.59% phosphoric acid, 0.27 mM EDTA, 8.9 mM sodium heptane sulfonic acid, and a flow rate of 0.5 mL/min. 3-HK was detected by an electrochemically detector (oxidation potential: +0.55 V; Cat# ECD-300; Eicom).

2.15 | Data analyses

All statistical analyses were performed using GraphPad Prism 6 Software (GraphPad Software Inc.). Significance was assessed using *t* tests, or in the case of multiple comparisons, an analysis of variance (ANOVA) with repeated measures. The Tukey–Kramer test was used for post hoc analyses when *F* ratios were significant. An assessment of the normality of the data prior to the statistical comparisons has not been carried out; however, this type of analysis was resistant to deviations from the assumptions of the traditional ordinary-least-squares ANOVA, and are robust to outliers, thus being insensitive to distributional assumptions (such as normality) (Huber, 1996). Data were not assessed for normality, and no test for outliers was conducted. The criterion for a significant difference was $p < .05$ for all statistical evaluations. All data are expressed as mean ± SEM.

3 | Results

3.1 | LPS triggers the development of depression-like and sickness behaviors

We induced acute depression-like symptom in mouse with intraperitoneal injection of LPS as described by Yamawaki et al. (2018). Mice were subjected to behavioral tests to investigate whether LPS-induced depression-like behavior 24 hr after injection. LPS significantly increased mouse immobility during the FST (Figure 1a; Student's *t* test, *t* = 3.058, df = 18, $^{**}p < .01$). Since LPS induces sickness behavior, such as a decrease in body weight and locomotor activity (Dantzer et al., 2008), mice were weighed before and 24 hr after the LPS injection. LPS significantly decreased body weight in mice compared to mice in the PBS group (Figure 1b; two-way ANOVA followed by Tukey's multiple comparison test, time [$F(1,36) = 3.564$, $p = .0671$], treatment [$F(1,36) = 35.01$, $^{**}p < .01$], time × treatment [$F(1,36) = 40.89$, $^{**}p < .01$]). During the OFT, LPS significantly decreased locomotor activity (Figure 1c; Student's *t* test, *t* = 5.594, df = 18, $^{**}p < .01$) and the number of rearing behaviors (Figure 1d; Student's *t* test, *t* = 4.373, df = 18, $^{**}p < .01$). However, there was no change in either index of anxiety in LPS group compared to PBS group: starting latency (Figure 1e; Student's *t* test, *t* = 0.6089, df = 18, $p = .55$) or time spent in the center or corner zone (Figure 1f; Student's *t* test, center [*t* = 1.189, df = 18, $p = .25$], corner [*t* = 0.3833, df = 18, $p = .76$]). A rotarod test was performed to investigate whether these LPS-induced behavioral changes were because of motor dysfunction. There was no difference observed in the duration of maintained balance between the LPS and PBS groups (Figure 1g; two-way ANOVA followed by

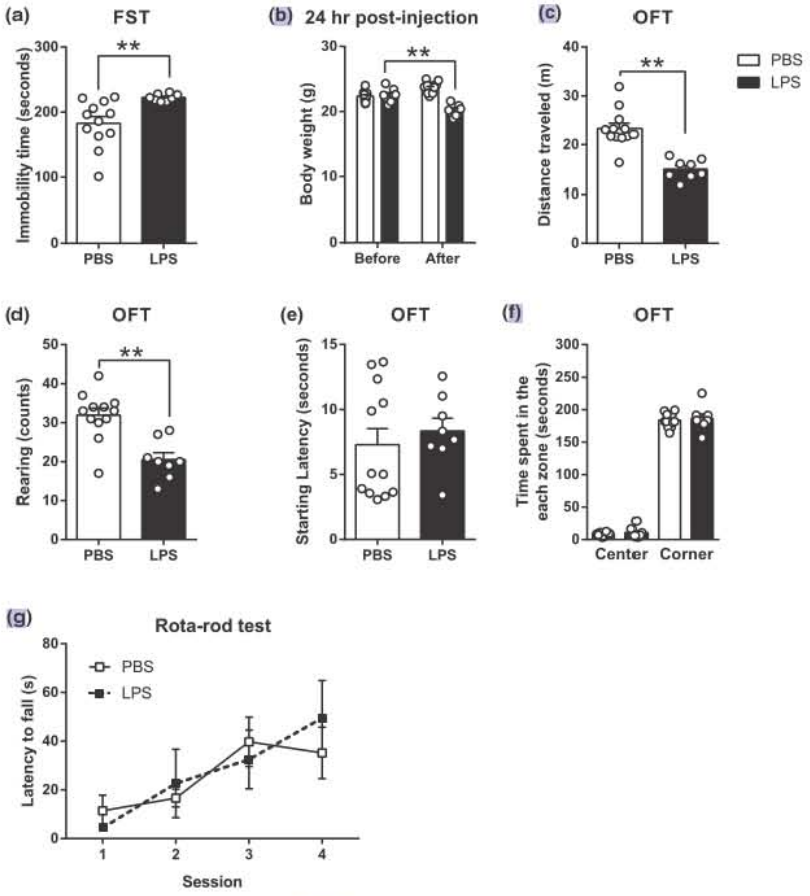

FIGURE 1 LPS triggers the development of depression and sickness behavior. (a) The FST was performed 24 hr after LPS injection (Student'sttest, $^{**}p < .01$;*n* = 8–12 mice in each group). (b) Body weight was measured before and 24 hr after LPS injection (two-way ANOVA followed by Tukey's multiple comparison test, time [$p > .05$], treatment [$^{**}p < .01$], time × treatment [$^{**}p < .01$];*n* = 8–12 mice in each group). (c–f) The OFT was performed 24 hr after LPS injection (*n* = 8–12 mice in each group). All data were analyzed with Student'sttest showing distance traveled (c,$^{**}p < .01$), rearing counts (d, $^{**}p < .01$), starting latency (e,$p > .05$), and time spent in the center and corner of the zone (f, center [$p > .05$], corner [$p > .05$];*n* = 8–12 mice in each group). (g) Rotarod test was performed 24 hr after LPS injection (two-way ANOVA followed by Tukey's multiple comparison test, session [$^{**}p < .01$], treatment [$p > .05$], session × treatment [$p > .05$];*n* = 8–10 mice in each group). All data are expressed as mean ± SEM

Tukey's multiple comparison test, session [$F(3,64) = 4.929$, $^{**}p < .01$], treatment [$F(1,64) = 0.04569$, $p = .8314$], session × treatment [$F(3,64) = 0.5570$, $p = .6453$]). These results suggest that acute LPS injection induces depression-like behavior and sickness behavior in mice without inducing anxiety or motor dysfunction.

3.2 | LPS up-regulates IDO1 expression in the PFC, but not in the HIP

IDO1 is essential for LPS-induced depression-like behavior in mice (O'Connor, et al., 2009). The increase in pro-inflammatory cytokines in the brain contributes to IDO1 up-regulation (Jo et al., 2015). The increased expression of pro-inflammatory cytokines such as IL-1β and TNF-α in the PFC and HIP were observed after LPS injection (Figures S2a,b,d,e; Student's *t* test, IL-1β in PFC [$t = 11.32$, df = 18, $^{**}p < .01$], TNF-α in PFC [$t = 9.363$, df = 18, $^{*}p < .01$], IL-1β in HIP [$t = 13.96$, df = 18, $^{**}p < .01$], TNF-α in HIP [$t = 15.24$, df = 18, $^{**}p < .01$]), but that of IL-6 was significantly decreased only in the PFC by qRT-PCR (Figures S2c,f; Student's *t* test, IL-6 in PFC [$t = 2.752$, df = 18, $^{*}p < .05$], IL-6 in HIP [$t = 1.356$, df = 18, $p = .19$]). To further investigate whether LPS-induced depression-like behavior is related to up-regulation of IDO1 in the brain, the expression of IDO1 mRNA and protein was examined in the mouse PFC and HIP by qRT-PCR and western blotting, respectively. Tissue samples were collected at 2, 6, 12, and 24 hr after LPS injection (Figure 2a). The mRNA level of IDO1 was up-regulated in the PFC between 6 hr and 24 hr after LPS injection (Figure 2b; two-way ANOVA followed by Tukey's multiple comparison test, $F(3,55) = 15.34$, $^{**}p < .01$). IDO1 mRNA levels in the HIP were up-regulated only 6 hr after LPS

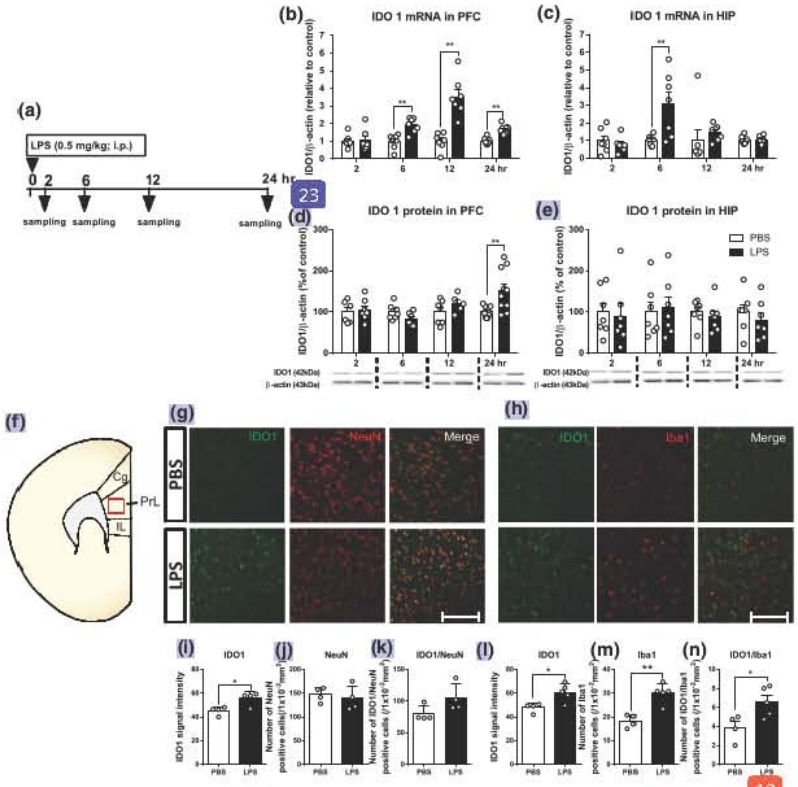

FIGURE 2 LPS up-regulates IDO1 expression in the PFC, but not in the HIP. (a) Experimental time course. (b, c) The mRNA levels of IDO1 were measured in the PFC (b) and HIP (c) at 2, 6, 12, and 24 hr after LPS injection by qRT-PCR (two-way ANOVA followed by Tukey's multiple comparison test, PFC [$^{**}p < .01$], HIP [$^{**}p < .01$];$n = 7$–10 mice in each group). (d, e) The protein levels of IDO1 were measured in the PFC (d) and HIP (e) at 2, 6, 12, and 24 hr after LPS injection by western blotting (two-way ANOVA followed by Tukey's multiple comparison test, PFC [$^{**}p < .01$], HIP [$p > .05$];$n = 7$–10 mice in each group). Data are normalized to the expression levels in the PBS group. (f) Schematic illustration showing the PFC section that was included in this analysis (Red dotted lines). (g, h) Representative images of double staining with anti-IDO1 (green) and anti-NeuN (g, red) or anti-Iba1 (h, red) in the PFC 24 hr after LPS injection. Scale bar: 100 μm. (i) IDO1 signal intensity and (j) NeuN-positive cells were measured in the PFC (Student's*t*test, IDO1 signal intensity [$^{*}p < .05$], NeuN-positive cells [$p > .05$];$n = 4$–5 mice in each group). (k) The number of IDO1/NeuN double-positive cells was quantified in the PFC (Student's*t*test,$p > .05$;$n = 4$–5 mice in each group). (l) IDO1 signal intensity and (m) Iba1-positive cells were measured in the PFC (Student's*t*test, IDO1 [$^{*}p < .05$], Iba1-positive cells [$^{**}p < .01$];$n = 4$–5 mice in each group). (n) The number of IDO1/Iba1 double positive cells was quantified in the PFC (Student's*t*test, $^{*}p < .05$;$n = 4$–5 mice in each group). The data are expressed as mean ± SEM. Cg, cingulate cortex; PrL, prelimbic cortex; IL, infralimbic cortex

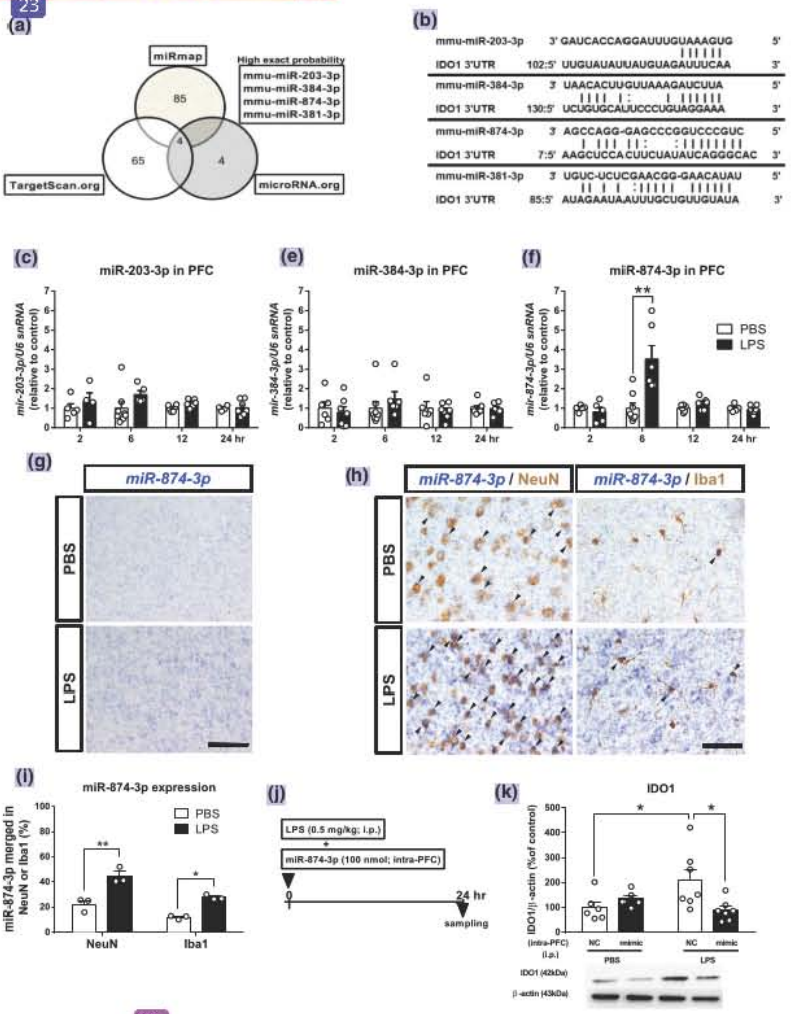

FIGURE 3 LPS transiently increases the expression of miR-874-3p in the PFC, and its over-expression down-regulates IDO1 protein level. (a) Predicted regulatory miRNAs to IDO1. The left middle panel represents the intersection of the three databases. The numbers in the panel indicate candidate miRNAs in each database. Four miRNAs that have a high probability of regulating IDO1 expression are shown in the right box. (b) Sequence alignment of the miR-203-3p, miR-384-3p, miR-874-3p, and miR-381-3p base-pairing site in the 3′ UTR of IDO1 mRNAs in mice. (c-e) The expression levels of miR-203-3p (c), miR-384-3p (d), and miR-874-3p (e) of the PFC were analyzed by qRT-PCR at 2, 6, 12, and 24 hr after LPS injection (two-way ANOVA followed by Tukey's multiple comparison test, miR-203-3p [$p > .05$], miR-384-3p [$p > .05$], miR-874-3p [$^{**}p < .01$];$n = 5$–8 mice in each group). (f) Representative images of *in situ* hybridization for miR-874-3p (blue) in the PFC 6 hr after LPS injection. Scale bar: 100 μm. (g) Double staining by *in situ* hybridization for miR-874-3p (blue) and immunostaining with anti-NeuN (brown) or anti-Iba1 (brown) in the PFC 6 hr after LPS injection. Arrowheads indicate double-positive cells for both miR-874-3p and NeuN or Iba1. Scale bar: 50 μm. (h) The percentage of miR-874-3p-positive cells expressing neuron or microglia marker was quantified in the PFC (Student's *t* test, NeuN [$^{**}p < .01$], Iba1 [$^{*}p < .05$];$n = 3$ mice in each group). (i) The experimental time course. (j) The protein level of IDO1 were examined in the PFC 24 hr after LPS injection followed by miR-874-3p mimic microinjection by western blotting (two-way ANOVA followed by Tukey's multiple comparison test, treatment [$p > .05$], microinjection [$p > .05$], treatment with microinjection [$^{**}p < .01$];$n = 6$–7 mice in each group). The data are expressed as mean ± SEM. NC, miR-negative control

injection (Figure 2c; two-way ANOVA followed by Tukey's multiple comparison test, $F(3,49) = 5.197$, $^{**}p < .01$). Moreover, the IDO1 protein level in the PFC was up-regulated 24 hr after LPS injection (Figure 2d; two-way ANOVA followed by Tukey's multiple comparison test, $F(3,49) = 3.880$, $^{**}p < .01$). However, the IDO1 protein level in the HIP was the same at all timepoints for the LPS and PBS groups (Figure 2e; two-way ANOVA followed by Tukey's multiple comparison test, $F(3,48) = 0.1675$, $p = .9178$). To confirm this result, the localization of IDO1 was determined by double immunostaining with IDO1 and NeuN (neuronal marker) or Iba1 (microglia marker) in the PFC (Figure 2f–h). Quantification data showed that IDO1 intensity was significantly higher in the IDO1/NeuN-stained samples in the

LPS-group (Figure 2i; Student's *t* test, $t = 3.023$, df = 6, $^{*}p < .05$). No differences were observed in the number of NeuN-positive cells (Figure 2j; Student's *t* test, $t = 0.5335$, df = 6, $p = .6129$) or IDO1/NeuN-double-positive cells between the LPS and PBS groups (Figure 2k; Student's *t* test, $t = 1.964$, df = 6, $p = .0972$). Similarly, the intensity of IDO1 was high in the IDO1/Iba1-stained samples in the LPS-group (Figure 2l; Student's *t* test, $t = 3.1$, df = 7, $^{*}p < .05$). The numbers of Iba1-positive cells (Figure 2m; Student's *t* test, $t = 4.8$, df = 7, $^{**}p < .01$) and IDO1/Iba1-double-positive cells (Figure 2n; Student's *t* test, $t = 2.716$ df = 7, $^{*}p < .05$) were also significantly increased in the LPS group. Quantification of Iba1 and PCNA (proliferation cell marker)-double-positive cells was significantly higher in the LPS-group (Figure S3a,d; Student's *t* test, $t = 18.51$, df = 7, $^{**}p < .01$). Co-localization of LPS-induced Iba1-positive cells with GFAP (astrocyte marker) and F4/80 (macrophage marker)-positive cells was not observed (Figure S3b,c). This suggested that these Iba1-positive cells reflect the microglial proliferation rather than the migration of macrophages and other cell types. These results proposed that LPS-induced depression-like behavior is likely related to up-regulation of IDO1 in both the neurons and microglia of the PFC.

3.3 | LPS transiently increases the expression of miR-874-3p in the PFC, and its over-expression down-regulates IDO1 protein level

MiRNAs regulate protein expression by targeting mRNA and may serve as a potential therapeutic target (O'Connor et al., 2012). To investigate whether miRNAs are involved in the regulation of IDO1 expression, three databases were employed to determine the candidate miRNAs. A total of 85 potential regulatory miRNAs were predicted from the miRmap, 65 from TargetScan, and four from the microRNA.org database. Four miRNAs (miR-203-3p, miR-384-3p, miR-874-3p, and miR-381-3p) were chosen for their high exact probability by Venn diagram analysis (Figure 3a). The interactions of IDO1 mRNA at the 3′ UTR are shown in Figure 3b. qRT-PCR was performed to confirm which miRNAs are important for LPS-induced up-regulation of IDO1 in the PFC. Among the miRNAs, miR-381-3p was not detectable in either the LPS or PBS groups. The expression levels of miR-203-3p and miR-384-3p did not differ at any timepoint between the LPS and PBS groups (Figures 3c,d; two-way ANOVA followed by Tukey's multiple comparison test, miR-203-3p [$F(3,37) = 0.735$, $p = .5378$], miR-384-3p [$F(3,46) = 0.6642$, $p = .5783$]). Importantly, the expression level of miR-874-3p was significantly up-regulated 6 hr after LPS injection (Figure 3e; two-way ANOVA followed by Tukey's multiple comparison test, $F(3,40) = 10.30$, $^{**}p < .01$). The increase in miR-874-3p expression after LPS injection was further confirmed by *in situ* hybridization (Figure 3f). The increase in miR-874-3p was observed in both NeuN- and Iba1-positive cells after LPS injection by double labeling of miR-874-3p and NeuN or Iba1 by *in situ* hybridization and immunostaining, respectively (Figures 3g,h; Student's *t* test, NeuN [$t = 1.759$, df = 4, $^{**}p < .01$], Iba1 [$t = 4.594$, df = 4, $^{*}p < .05$]). Altogether, miR-874-3p may play an important role in LPS-induced up-regulation of IDO1 in the PFC. To further confirm its role in the regulation of IDO1 levels, mice were injected with LPS (0.5 mg/kg) and then immediately infused miR-NC or miR-874-3p mimic into the PFC (Figure 3i and Figure S4a). MiR-874-3p prevented the increase in IDO1 mRNA and protein levels in the PFC 24 hr after LPS injection as seen by qRT-PCR and western blotting, respectively (Figure S3j and S4b; two-way ANOVA followed by Tukey's multiple comparison test, IDO1 mRNA (treatment [$F(1,26) = 28.33$, $^{**}p < .01$], microinjection [$F(1,26) = 8.624$, $^{**}p < .01$], treatment with microinjection [$F(1,26) = 4.474$, $^{*}p < .05$]; IDO1 protein (treatment [$F(1,21) = 1.445$, $p = .2427$], microinjection [$F(1,21) = 2.664$, $p = .1176$], treatment with microinjection [$F(1,21) = 8.067$, $^{**}p < .01$]). Toll-like receptor 4 (TLR4) is known as an LPS receptor and induces pro-inflammatory cytokines (De Paola et al., 2012). To examine the potential off-target effects of miR-874-3p, we measured the expression of TLR4 and pro-inflammatory cytokines. MiR-874-3p failed to affect the expression of TLR4, IL-1β, TNF-α, and IL-6 in the PFC (Figure S5; two-way ANOVA followed by Tukey's multiple comparison test, TLR4 (treatment [$F(1,28) = 0.1314$, $p = .7197$], microinjection [$F(1,28) = 0.8784$, $p = .3566$], treatment with microinjection [$F(1,28) = 0.3011$, $p = .3911$]), IL-1β (treatment [$F(1,26) = 18.12$, $^{**}p < .01$], microinjection [$F(1,26) = 0.2110$, $p = .6498$], treatment with microinjection [$F(1,26) = 6.915$, $^{*}p < .05$]), TNF-α (treatment [$F(1,26) = 31.06$, $^{**}p < .01$], microinjection [$F(1,26) = 2.847$, $p = .1035$], treatment with microinjection [$F(1,26) = 0.0000677$, $p = .9934$]), IL-6 (treatment [$F(1,26) = 0.06351$, $p = .8030$], microinjection [$F(1,26) = 0.1989$, $p = .6593$], treatment with microinjection [$F(1,26) = 2.806$, $p = .1059$]). These results suggest that miR-874-3p regulates IDO1 protein levels after LPS injection.

3.4 | Microinjection of 1-MT or miR-874-3p mimic into the PFC improves LPS-induced depression-like behavior

It has been suggested that miRNAs are novel targets of therapeutic strategies for depression-like behavior in animal models (Deng et al., 2019; Lopizzo et al., 2019; O'Connor et al., 2012). Therefore, we speculated that the inhibition of IDO1 in the PFC by miR-874-3p mimic might have a preventive effect on LPS-induced depression-like behavior in mice. First, we infused 1-MT, a potent IDO1 antagonist, into the PFC of the LPS group and subjected the mouse to OFT and FST 24 hr after the LPS injection (Figure 4a). Intra-PFC infusion of 1-MT prevented the increase in immobility in the FST of the LPS group (Figure 4b; two-way ANOVA followed by Tukey's multiple comparison test, treatment [$F(1,35) = 3.429$, $p = .0725$], microinjection [$F(1,35) = 7.136$, $p = .0114$], treatment with microinjection [$F(1,35) = 4.415$, $^{*}p < .05$]). However, 1-MT failed to prevent the decrease in distance traveled (Figure 4c; two-way ANOVA followed by Tukey's multiple comparison test, treatment [$F(1,35) = 15.26$, $^{**}p < .01$], microinjection [$F(1,35) = 1.137$, $p = .2935$], treatment with microinjection [$F(1,35) = 0.04056$, $^{*}p < .05$]) and number of rearing behaviors in

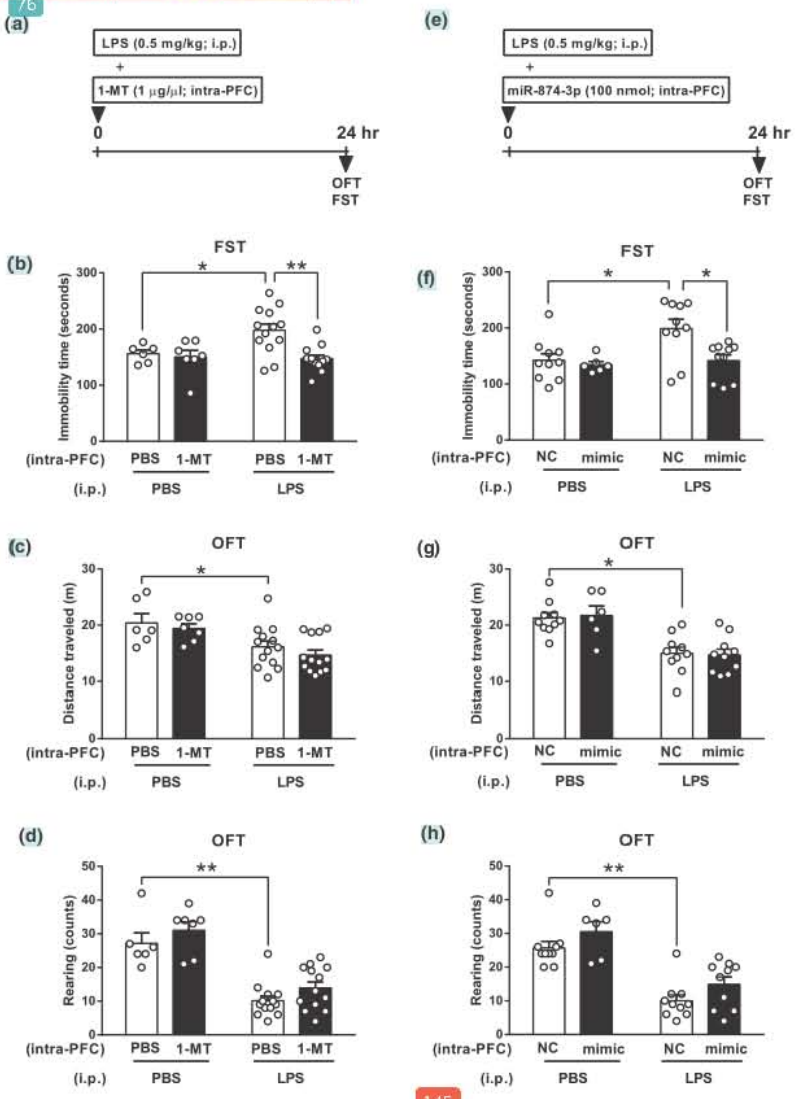

FIGURE 4 Microinjection of 1-MT or miR-874-3p mimic into the PFC improves LPS-induced depression-like behavior. (a) The 1-MT microinjection time course. (b) The FST was performed 24 hr after LPS injection followed by 1-MT microinjection into the PFC (two-way ANOVA followed by Tukey's multiple comparison test, treatment [$p > .05$], microinjection [$p > .05$], treatment with microinjection [$^{*}p < .05$];$n = 7$–13 mice in each group). (c-d) The OFT was performed 24 hr after LPS injection followed by 1-MT microinjection into PFC (two-way ANOVA followed by Tukey's multiple comparison test showing distance traveled (c) (treatment [$^{**}p < .01$], microinjection [$p > .05$], treatment with microinjection [$^{*}p < .05$];$n = 7$–13 mice in each group) and rearing (d) (treatment [$^{**}p < .01$], microinjection [$p > .05$], treatment with microinjection [$p > .05$];$n = 7$–13 mice in each group). (e) The miR-874-3p microinjection time course. (f) The FST was performed 24 hr after LPS injection followed by miR-874-3p mimic microinjection in the PFC (two-way ANOVA followed by Tukey's multiple comparison test, treatment [$^{*}p < .05$], microinjection [$^{*}p < .05$], treatment with microinjection [$^{*}p < .05$];$n = 6$–10 mice in each group). (g-h) The OFT was performed 24 hr after LPS injection followed by miR-874-3p mimic microinjection into the PFC (two-way ANOVA followed by Tukey's multiple comparison test showing distance traveled (g) (treatment [$^{**}p < .01$], microinjection [$p > .05$], treatment with microinjection [$p > .05$];$n = 6$–10 mice each) and rearing (h) (treatment [$^{**}p < .01$], microinjection [$^{*}p < .05$], treatment with microinjection [$p > .05$];$n = 6$-10 mice in each group). The data are expressed as mean ± SEM. 1-MT, 1-methyl-*l*-tryptophan; NC, miR-negative control

the OFT (Figure 4d; two-way ANOVA followed by Tukey's multiple comparison test, treatment [$F(1,35) = 64.95$, $^{**}p < .01$], microinjection [$F(1,35) = 3.230$, $p = .0809$], treatment with microinjection [$F(1,35) = 0.0002297$, $p = .9880$]). In a separate experiment, the increase in IDO1 level was inhibited by over-expression of miR-874-3p in the PFC of the LPS group (Figure 3j). In a similar way, the miR-874-3p mimic was infused into the PFC of the LPS group and conducted OFT and FST 24 hr later (Figure 4e). Interestingly, the increase in immobility in the FST of the LPS group was also prevented by the miR-874-3p mimic infusion (Figure 4f; two-way

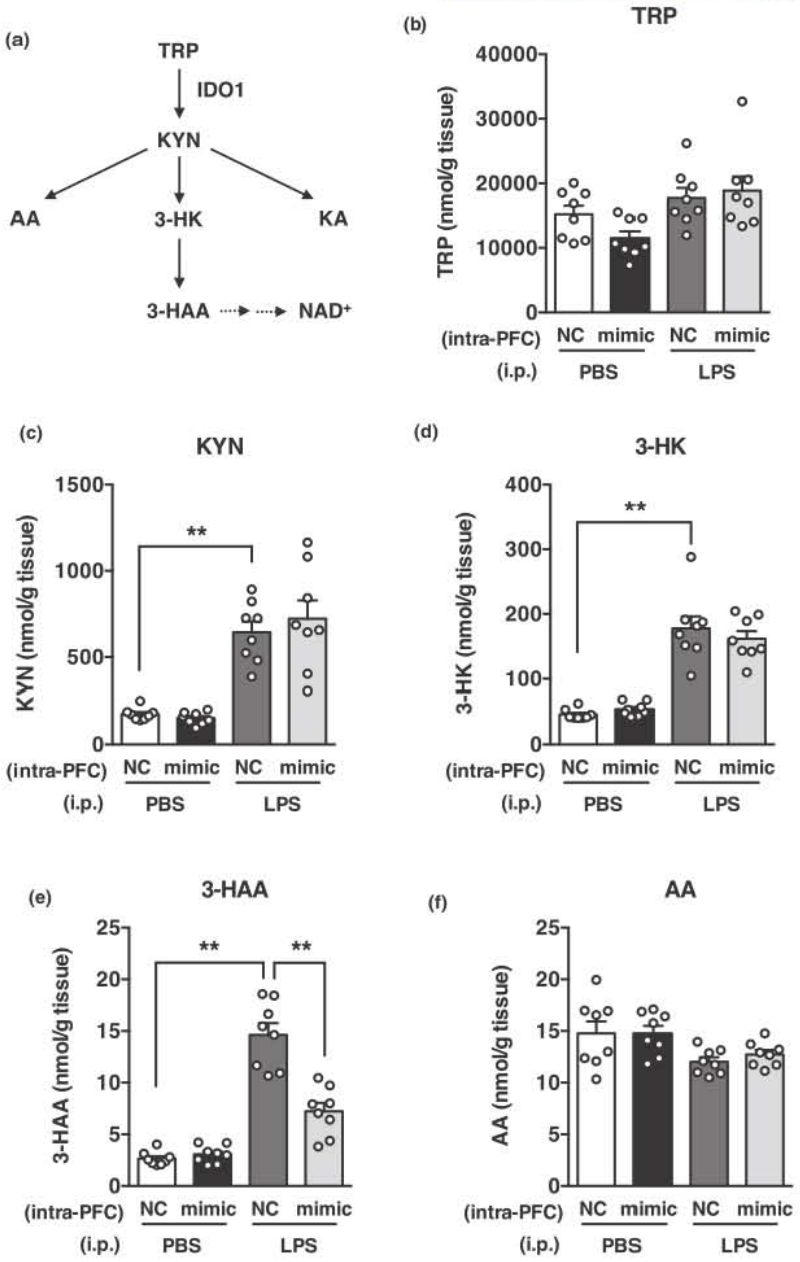

FIGURE 5 Microinjection of miR-874-3p mimic into the PFC improves the levels of 3-HAA. (a) Schematic of KYN metabolism. (b-f) The concentrations of TRP (b), KYN (c), 3-HK (d), 3-HAA (e) and AA (f) were measured 24 hr after LPS injection followed by miR-874-3p mimic microinjection into PFC 4by HPLC (two-way ANOVA followed by Tukey's multiple comparison test, TRP (treatment [$^{**}p < .01$], microinjection [$p > .05$], treatment with microinjection [$p > .05$]), KYN (treatment [$^{**}p < .01$], microinjection [$p > .05$], treatment with microinjection [$p > .05$]), 3-HK (treatment [$^{**}p < .01$], microinjection [$p > .05$], treatment with microinjection [$p > .05$], 3-HAA (treatment [$^{**}p < .01$], microinjection [$^{**}p < .01$], treatment with microinjection [$^{**}p < .01$], AA (treatment [$^{**}p < .01$], microinjection [$p > .05$], treatment with microinjection [$p > .05$]);$n = 8$ mice in each group). The data are expressed as mean ± SEM. TRP, tryptophan; KYN, kynurenine; 3-HK, 3-hydroxykynurenine; KA, kynurenic acid; AA, anthranilic acid; 3-HAA, 3-hydroxy anthranilic acid; NAD^+, nicotinamide adenine dinucleotide; NC, miR-negative control

ANOVA followed by Tukey's multiple comparison test, treatment [$F(1,34) = 6.246$, $^{*}p < .05$], microinjection [$F(1,34) = 7.146$, $^{*}p < .05$], treatment with microinjection [$F(1,34) = 4.176$, $^{*}p < .05$]). In contrast, similar to the results of 1-MT, the miR-874-3p mimic infusion failed to prevent the decrease in the distance traveled (Figure 4g; two-way ANOVA followed by Tukey's multiple comparison test, treatment [$F(1,32) = 33.22$, $^{**}p < .01$], microinjection [$F(1,32) = 0.004486$, $p = .9470$], treatment with microinjection [$F(1,32) = 0.1119$, $p = .7401$]) and number of rearing behaviors (Figure 4h; two-way ANOVA followed by Tukey's multiple comparison, treatment [$F(1,32) = 50.80$, $^{**}p < .01$], microinjection [$F(1,32) = 4.879$, $^{*}p < .05$], treatment with microinjection [$F(1,32) = 0.0005185$, $p = .9820$] in the OFT. There was no difference observed in the time spent of the center or corner zone after 1-MT and miR-874-3p mimic infusion (Figure S6; two-way ANOVA followed by Tukey's multiple comparison test, center with 1-MT (treatment [$F(1,35) = 1.994$, $p = .1668$], microinjection [$F(1,35) = 6.214$, $^{*}p < .05$], treatment × microinjection [$F(1,35) = 0.0003981$, $p = .9842$]), corner with 1-MT (treatment [$F(1,32) = 2.597$, $p = .1169$], microinjection [$F(1,32) = 0.3040$, $p = .5852$], treatment × microinjection [$F(1,32) = 0.6193$, $p = .4371$], center with miR-873-3p (treatment [$F(1,32) = 1.295$, $p = .2635$], microinjection [$F(1,32) = 0.5918$, $p = .5918$], treatment × microinjection [$F(1,32) = 0.08959$, $p = .7666$]), corner with miR-873-3p (treatment [$F(1,35) = 1.721$, $p = .1981$], microinjection [$F(1,35) = 3.445$, $p = .0719$], treatment × microinjection [$F(1,35) = 0.01696$, $p = .8971$]). Collectively, these data suggest that microinjection of miR-874-3p into the PFC prevents LPS-induced depression-like behavior, but not sickness behavior, through suppression of IDO1 activity.

3.5 | Microinjection of miR-874-3p mimic into the PFC improves the levels of 3-HAA

IDO1-mediated activation of KYN pathway is related to depressive-like symptoms in mice (O'Connor, et al., 2009). To further investigate the effects of miR-874-3p on the KYN pathway, we infused an miR-874-3p mimic into the PFC of the LPS group and measured the concentrations of KYN metabolites (TRP, KYN, 3-HK, KA, 3-HAA, and AA; Figure 5a) in the PFC by HPLC. Among the KYN metabolites, KA was not detectable in either the PBS or LPS groups. Compared to the PBS group, the levels of KYN, 3-HK, and 3-HAA but not TRP or AA were significantly increased in the LPS group (Figure 5b–f; two-way ANOVA followed by Tukey's multiple comparison test, TRP (treatment [$F(1,28) = 9.573$, $^{**}p < .01$], microinjection [$F(1,28) = 0.6610$, $p = .4231$], treatment with microinjection [$F(1,28) = 2.298$, $p = .1407$]), KYN (treatment [$F(1,28) = 70.45$, $^{**}p < .01$], microinjection [$F(1,28) = 0.2079$, $p = .6519$], treatment with microinjection [$F(1,28) = 0.6644$, $p = .4214$]), 3-HK (treatment [$F(1,28) = 112.0$, $^{**}p < .01$], microinjection [$F(1,28) = 0.1279$, $p = .7233$], treatment with microinjection [$F(1,28) = 1.128$, $p = .2973$], 3-HAA (treatment [$F(1,28) = 121.9$, $^{**}p < .01$], microinjection [$F(1,28) = 22.87$, $^{**}p < .01$], treatment with microinjection [$F(1,28) = 28.59$, $^{**}p < .01$], AA (treatment [$F(1,28) = 10.22$, $^{**}p < .01$], microinjection [$F(1,28) = 0.2287$, $p = .6362$], treatment with microinjection [$F(1,28) = 0.2287$, $p = .6362$])). The miR-874-3p mimic potently reduced 3-HAA levels (Figure 5e), whereas KYN and 3-HK remained unchanged compared to miR-NC group (Figure 5c,d). These results suggest that the beneficial effect of miR-874-3p on LPS-induced depression-like behavior may be associated with reduced 3-HAA levels.

4 | Discussion

In this study, we showed that LPS-induced depression-like behavior was related to increase in IDO1 expression in the PFC. Our data confirmed that IDO1 is an important regulator of depression-like behavior induced by LPS, since pharmacological inhibition of IDO1 by 1-MT protected mice from LPS-induced depression-like behavior. Furthermore, microinjection of miR-874-3p into the PFC also reversed depression-like behavior through a decrease in IDO1 protein levels. The limitation of our study is because of the nature of the acute inflammatory stimulus that caused inflammation-induced depression. LPS-induced depression-like behavior recapitulates the main features of inflammation-induced depression but lacks the chronicity that is characteristic of MDD. In fact, the expression of miR-874-3p was changed in the mice exposed to chronic social defeated stress (unpublished data). Although further validation using other depression models is needed, this is the first report to provide new insight for miRNA-874-3p as a potential therapeutic target for MDD.

In a previous study, mice injected with LPS were originally developed as an animal model for sickness behavior characterized by decrease in body weight, food intake, and exploratory activity. This behavior resulted from the production of pro-inflammatory cytokines in the periphery and brain (Dantzer et al., 2008). We found that the direct inhibition of IDO1 in the PFC suppressed the increase in immobility in the FST, but not the decrease in open-field activity, in the LPS group. These data suggest that IDO1 selectively related to inflammation-induced depression-like behavior, but not anxiety or sickness behavior. Our finding is consistent with a previous study that showed a different pathogenesis of sickness and depression-like behavior after LPS injection (O'Connor, et al., 2009).

Previous reports have indicated that change in miRNA levels in the brain may significantly contribute to the development of depression in animal models (Deng et al., 2019; Lo Iacono et al., 2019; Lou et al., 2019). Using Venn diagram analysis from three databases, we identified miR-203-3p, miR-384-3p, miR-874-3p, and miR-381-3p as the regulator of IDO1 expression at the 3′ UTR. Among them, miR-874-3p was significantly up-regulated after LPS injection. However, there are no reports on the role of miR-874-3p in the pathogenesis of MDD. In some cancers, miR-874-3p can act as a tumor suppressor (Han et al., 2016). Importantly, other studies have indicated that up-regulated miR-874-3p increases proliferation and suppresses apoptosis of neurons by inhibiting an apoptotic pathway in cerebral

ischemia models (Jiang et al., 2018). IDO1 is elevated in mice with cerebral ischemia and correlates with increased risk of death (Jackman et al., 2011). IDO1-derived KYN metabolites can promote apoptosis in some types of cells *in vitro* and *in vivo* (Morita et al., 2001). We found that IDO1 was up-regulated in the PFC after LPS injection. Microinjection of miR-874-3p into the PFC down-regulates LPS-induced IDO1 expression and prevents the LPS-induced increase in immobility in the FST. These results suggest that miR-874-3p also exerted protective roles against LPS-induced depression-like behavior by suppressing an apoptotic pathway via IDO1 inhibition.

It is well known that LPS-induced inflammatory response in the CNS is dependent on TLR4 (Singhal & Baune, 2017; Walter et al., 2007). TLR4 is expressed in both microglia and neuron (De Paola et al., 2012) and involved in the proliferation and differentiation of the cells (Leitner et al., 2019; Rolls et al., 2007). We demonstrated that an increase in Iba1-positive cells after LPS injection reflects the microglial proliferation rather than the migration of macrophage and other cell types. Our results suggest that the microglial proliferation was increased because of TLR4 activation in the LPS-treated mice. Furthermore, we found that IDO1 and miR-874-3p express not only in microglia but also in neuron after LPS injection. Although the precise molecular mechanisms are not yet clear, it is possible that IDO1, localized to the neurons, contributes to the development of depression-like behavior. Further studies on IDO1 deficiency in a specific cell subset will provide important insights into the role of IDO1 in the pathogenesis of MDD.

During inflammation, IDO1 and TDO are the major enzymes that metabolizes TRP in the KYN pathway (Fujigaki et al., 2017). The increase in IDO1 enzymatic activity is correlated with inflammation-associated depression (Dantzer et al., 2008; Murakami et al., 2016). We demonstrated that microinjection of 1-MT into PFC could partially reverse LPS-induced depressive-like states in mice. The behavioral effects of 1-MT could not be explained by the inhibition of the TDO as 1-MT has been shown to specifically act on IDO1 (O'Connor, et al., 2009). These findings suggest that IDO1 activation is an important feature of depressive-like states induced by inflammatory processes. Preclinical, *in vitro*, and postmortem data have demonstrated that elevation of KYN metabolites levels is also associated with neuronal damage and/or suppression of neurogenesis (Fischer et al., 2015). We demonstrated that LPS disturbed KYN metabolites in the PFC. LPS did not affect the TRP and AA levels; meanwhile, KYN, 3-HK, and 3-HAA were increased in LSP-injected mice. Of note, miR-874-3p strongly inhibits LPS-induced 3-HAA, whereas no difference was observed in KYN and 3-HK levels. It has been recognized that 3-HAA generates the potent oxidative species superoxide (O_2^-), hydroxyl radical (HO^-) and hydrogen peroxide (H_2O_2), which frequently contribute to increased apoptosis (Smith et al., 2009). In line with these data, 3-HAA induced neuronal cell death with apoptotic features following generation of ROS in primary neurons (Stone & Darlington, 2002). Recent studies have identified neuronal apoptosis and reduced volume of frontal cortex in patients with MDD (Lucassen et al., 2001; McKernan et al., 2009; Shelton et al., 2011). Although additional experiments were necessary to fully understand the role of 3-HAA and in LPS-induced behavioral changes, 3-HAA may be responsible for LPS-induced depression-like behavior. Aside from IDO1, these data suggested that other rate limiting enzymes or downstream KYN metabolites were also responsible for LPS-induced depression-like behavior. In fact, LPS increased the expression of kynrenine-3-monooxy-genase (KMO), and IDO1 was observed in the rats after systemic administration (Connor et al., 2008).

In summary, our data indicated two findings. First, LPS-induced depression-like behavior is related to an increase in IDO1 expression in the PFC. Second, IDO1 inhibition by miR-874-3p or IDO1 antagonist via intra-PFC infusions can reverse depression-like behavior in mice. Our data implicate IDO1 in the PFC as an important component of LPS-induced depression-like behavior. Moreover, miR-874-3p exerted antidepressant-like effects by down-regulating IDO1 in the PFC. These findings suggest that miR-874-3p may suppress the pathophysiology of MDD by inhibiting IDO1 expression. The beneficial effects of miR-874-3p were might be the consequence of suppressed LPS-induced 3-HAA levels. Our study provides the first insight into miR-874-3p as a novel potential therapeutic target for MDD.

ACKNOWLEDGMENTS

No financial or non-financial interests in relation to the work described in this manuscript is declared by the authors. This work was supported by Grants-in-Aid for Scientific Research from the Japan Society for the Promotion of Science (17H04252, 17K01969, 18K15377, 18K19761, and 19K07490) and by the Private University Research Branding Project from the Ministry of Education, Culture, Sports, Science and Technology of Japan (MEXT). This work was supported by a grant from the Education and Research Facility of Animal Models for Human Disease of the Fujita Health University. We thank our lab members for the helpful discussions. The authors declare no conflict of interest.

All experiments were conducted in compliance with the ARRIVE guidelines.

AUTHORS' CONTRIBUTIONS

WJS designed the project and the main conceptual ideas. participated in all experiments, and wrote the manuscript. KK supervised the work and wrote the manuscript. YW, AK, TI, and SF assisted with experiments. HF, YY, AJT, and KS contributed to the manuscript discussion. AM and TN supervised the work and finalized the manuscript.

ORCID

Kazuo Kunisawa https://orcid.org/0000-0002-4786-9681
Akihiro Mouri https://orcid.org/0000-0003-3833-4041

REFERENCES

Badawy, A. A. (2017). Kynurenine Pathway of Tryptophan Metabolism: Regulatory and Functional Aspects. *International Journal of Tryptophan Research*,*10*, 1178646917691938.

Bartel, D. P. (2004). MicroRNAs: genomics, biogenesis, mechanism, and function. *Cell*, *116*, 281–297.

Benton, T., Staab, J., & Evans, D. L. (2007). Medical co-morbidity in depressive disorders. *Annals of Clinical Psychiatry*, *19*, 289–303.

Bradley, K. A., Case, J. A., Khan, O., Ricart, T., Hanna, A., Alonso, C. M., & Gabbay, V. (2015). The role of the kynurenine pathway in suicidality in adolescent major depressive disorder. *Psychiatry Research*, *227*, 206–212.

Brites, D., & Fernandes, A. (2015). Neuroinflammation and depression: Microglia activation, extracellular microvesicles and microRNA dysregulation. *Frontiers in Cellular Neuroscience*, *9*, 476.

Cai, Y., Yu, X., Hu, S., & Yu, J. (2009). A brief review on the mechanisms of miRNA regulation. *Genomics Proteomics Bioinformatics*, *7*, 147–154.

Connor, T. J., Starr, N., O'Sullivan, J. B., & Harkin, A. (2008). Induction of indolamine 2,3-dioxygenase and kynurenine 3-monooxygenase in rat brain following a systemic inflammatory challenge: a role for IFN-gamma? *Neuroscience Letters*, *441*, 29–34.

Dantzer, R., O'Connor, J. C., Freund, G. G., Johnson, R. W., & Kelley, K. W. (2008). From inflammation to sickness and depression: when the immune system subjugates the brain. *Nature Reviews Neuroscience*, *9*, 46–56.

De Paola, M., Mariani, A., Bigini, P., Peviani, M., Ferrara, G., Molteni, M., Gemma, S., Veglianese, P., Castellaneta, V., Boldrin, V., Rossetti, C., Chiabrando, C., Forloni, G., Mennini, T., & Fanelli, R. (2012). Neuroprotective effects of toll-like receptor 4 antagonism in spinal cord cultures and in a mouse model of motor neuron degeneration. *Molecular Medicine*, *18*, 971–981.

Deng, Z. F., Zheng, H. L., Chen, J. G., Luo, Y., Xu, J. F., Zhao, G., Lu, J. J., Li, H. H., Gao, S. Q., Zhang, D. Z., & Zhu, L. Q. (2019). miR-214-3p targets beta-catenin to regulate depressive-like behaviors induced by chronic social defeat stress in mice. *Cerebral Cortex*, *29*, 1509–1519.

Dwivedi, Y. (2014). Emerging role of microRNAs in major depressive disorder: diagnosis and therapeutic implications. *Dialogues in Clinical Neuroscience*, *16*, 43–61.

Fava, M., & Davidson, K. G. (1996). Definition and epidemiology of treatment-resistant depression. *Psychiatric Clinics of North America*, *19*, 179–200.

Fischer, C. W., Eskelund, A., Budac, D. P., Tillmann, S., Liebenberg, N., Elfving, B., & Wegener, G. (2015). Interferon-alpha treatment induces depression-like behaviour accompanied by elevated hippocampal quinolinic acid levels in rats. *Behavioural Brain Research*, *293*, 166–172.

Flint, J., & Kendler, K. S. (2014). The genetics of major depression. *Neuron*, *81*, 484–503.

Fujigaki, H., Yamamoto, Y., & Saito, K. (2017). L-Tryptophan-kynurenine pathway enzymes are therapeutic target for neuropsychiatric diseases: Focus on cell type differences. *Neuropharmacology*, *112*, 264–274.

Han, J., Liu, Z., Wang, N., & Pan, W. (2016). MicroRNA-874 inhibits growth, induces apoptosis and reverses chemoresistance in colorectal cancer by targeting X-linked inhibitor of apoptosis protein. *Oncology Reports*, *36*, 542–550.

Holmes, S. E., Hinz, R., Conen, S., Gregory, C. J., Matthews, J. C., Anton-Rodriguez, J. M., Gerhard, A., & Talbot, P. S. (2018). Elevated translocator protein in anterior cingulate in major depression and a role for inflammation in suicidal thinking: A positron emission tomography study. *Biological Psychiatry*, *83*, 61–69.

Huber, P. J. (1996) Robust statistical procedures, Vol. 68: CBMS-NSF regional conference series in applied mathematics. Society for Industrial and Applied Mathematics, .

Iida, R., Yamada, K., Mamiya, T., Saito, K., Seishima, M., & Nabeshima, T. (1999). Characterization of learning and memory deficits in C57BL/6 mice infected with LP-BM5, a murine model of AIDS. *Journal of Neuroimmunology*, *95*, 65–72.

Jackman, K. A., Brait, V. H., Wang, Y., Maghzal, G. J., Ball, H. J., McKenzie, G., De Silva, T. M., Stocker, R., & Sobey, C. G. (2011). Vascular expression, activity and function of indoleamine 2,3-dioxygenase-1 following cerebral ischaemia-reperfusion in mice. *Naunyn-Schmiedeberg's Archives of Pharmacology*, *383*, 471–481.

Jiang, D., Sun, X., Wang, S., & Man, H. (2019). Upregulation of miR-874-3p decreases cerebral ischemia/reperfusion injury by directly targeting BMF and BCL2L13. *Biomedicine & Pharmacotherapy*, *117*, 108941.

Jo, W. K., Zhang, Y., Emrich, H. M., & Dietrich, D. E. (2015). Glia in the cytokine-mediated onset of depression: fine tuning the immune response. *Frontiers in Cellular Neuroscience*, *9*, 268.

Karthikeyan, A., Patnala, R., Jadhav, S. P., Eng-Ang, L., & Dheen, S. T. (2016). MicroRNAs: Key players in microglia and astrocyte mediated inflammation in CNS pathologies. *Current Medicinal Chemistry*, *23*, 3528–3546.

Krutzfeldt, J., Rajewsky, N., Braich, R., Rajeev, K. G., Tuschl, T., Manoharan, M., & Stoffel, M. (2005). Silencing of microRNAs in vivo with 'antagomirs'. *Nature*, *438*, 685–689.

Kunisawa, K., Kido, K., Nakashima, N., Matsukura, T., Nabeshima, T., & Hiramatsu, M. (2017). Betaine attenuates memory impairment after water-immersion restraint stress and is regulated by the GABAergic neuronal system in the hippocampus. *European Journal of Pharmacology*, *796*, 122–130.

Kunisawa, K., Shimizu, T., Kushima, I., Aleksic, B., Mori, D., Osanai, Y., Kobayashi, K., Taylor, A. M., Bhat, M. A., Hayashi, A., Baba, H., Ozaki, N., & Ikenaka, K. (2018). Dysregulation of schizophrenia-related aquaporin 3 through disruption of paranode influences neuronal viability. *Journal of Neurochemistry*, *147*, 395–408.

Lawson, M. A., Parrott, J. M., McCusker, R. H., Dantzer, R., Kelley, K. W., & O'Connor, J. C. (2013). Intracerebroventricular administration of lipopolysaccharide induces indoleamine-2,3-dioxygenase-dependent depression-like behaviors. *Journal of Neuroinflammation*, *10*, 87.

Leitner, G. R., Wenzel, T. J., Marshall, N., Gates, E. J., & Klegeris, A. (2019). Targeting toll-like receptor 4 to modulate neuroinflammation in central nervous system disorders. *Expert Opinion on Therapeutic Targets*, *23*, 865–882.

Lo Iacono, L., Ielpo, D., Accoto, A., Di Segni, M., Babicola, L., D'Addario, S. L., Ferlazzo, F., Pascucci, T., Ventura, R., & Andolina, D. (2019). MicroRNA-34a regulates the depression-like behavior in mice by modulating the expression of target genes in the dorsal raphe. *Molecular Neurobiology*, *57*, 823–836.

Lopizzo, N., Zonca, V., Cattane, N., Pariante, C. M., & Cattaneo, A. (2019). miRNAs in depression vulnerability and resilience: Novel targets for preventive strategies. *Journal of Neural Transmission*, *126*, 1241–1258.

Lou, D., Wang, J., & Wang, X. (2019). miR-124 ameliorates depressive-like behavior by targeting STAT3 to regulate microglial activation. *Molecular and Cellular Probes*, *48*, 101470.

Lucassen, P. J., Muller, M. B., Holsboer, F., Bauer, J., Holtrop, A., Wouda, J., Hoogendijk, W. J., De Kloet, E. R., & Swaab, D. F. (2001). Hippocampal apoptosis in major depression is a minor event and absent from subareas at risk for glucocorticoid overexposure. *The American Journal of Pathology*, *158*, 453–468.

Maes, M., Bosmans, E., De Jongh, R., Kenis, G., Vandoolaeghe, E., & Neels, H. (1997). Increased serum IL-6 and IL-1 receptor antagonist concentrations in major depression and treatment resistant depression. *Cytokine*, *9*, 853–858.

Maes, M., Leonard, B. E., Myint, A. M., Kubera, M., & Verkerk, R. (2011). The new '5-HT' hypothesis of depression: cell-mediated immune activation induces indoleamine 2,3-dioxygenase, which leads to lower plasma tryptophan and an increased synthesis of detrimental tryptophan catabolites (TRYCATs), both of which contribute to the onset of depression. *Progress in Neuro-Psychopharmacology and Biological Psychiatry*, *35*, 702–721.

McKernan, D. P., Dinan, T. G., & Cryan, J. F. (2009). "Killing the Blues": A role for cellular suicide (apoptosis) in depression and the antidepressant response? *Progress in Neurobiology*, *88*, 246–263.

McKinnon, M. C., Yucel, K., Nazarov, A., & MacQueen, G. M. (2009). A meta-analysis examining clinical predictors of hippocampal volume in patients with major depressive disorder. *Journal of Psychiatry & Neuroscience*, *34*, 41–54.

Miwa, M., Tsuboi, M., Noguchi, Y., Enokishima, A., Nabeshima, T., & Hiramatsu, M. (2011). Effects of betaine on lipopolysaccharide-induced memory impairment in mice and the involvement of GABA transporter 2. *Journal of Neuroinflammation*, *8*, 153.

Morita, T., Saito, K., Takemura, M., Maekawa, N., Fujigaki, S., Fujii, H., Wada, H., Takeuchi, S., Noma, A., & Seishima, M. (2001). 3-Hydroxyanthranilic acid, an L-tryptophan metabolite, induces apoptosis in monocyte-derived cells stimulated by interferon-gamma. *Annals of Clinical Biochemistry*, *38*, 242–251.

Mouillet-Richard, S., Baudry, A., Launay, J. M., & Kellermann, O. (2012). MicroRNAs and depression. *Neurobiology of Disease*, *46*, 272–278.

Mouri, A., Sasaki, A., Watanabe, K., Sogawa, C., Kitayama, S., Mamiya, T., Miyamoto, Y., Yamada, K., Noda, Y., & Nabeshima, T. (2012). MAGE-D1 regulates expression of depression-like behavior through serotonin transporter ubiquitylation. *Journal of Neuroscience*, *32*, 4562–4580.

Mouri, A., Ukai, M., Uchida, M., Hasegawa, S., Taniguchi, M., Ito, T., Hida, H., Yoshimi, A., Yamada, K., Kunimoto, S., Ozaki, N., Nabeshima, T., & Noda, Y. (2018). Juvenile social defeat stress exposure persistently impairs social behaviors and neurogenesis. *Neuropharmacology*, *133*, 23–37.

Murai, R., Noda, Y., Matsui, K., Kamei, H., Mouri, A., Matsuba, K., Nitta, A., Furukawa, H., & Nabeshima, T. (2007). Hypofunctional glutamatergic neurotransmission in the prefrontal cortex is involved in the emotional deficit induced by repeated treatment with phencyclidine in mice: implications for abnormalities of glutamate release and NMDA-CaMKII signaling. *Behavioural Brain Research*, *180*, 152–160.

Murakami, Y., Ishibashi, T., Tomita, E., Imamura, Y., Tashiro, T., Watcharanurak, K., Nishikawa, M., Takahashi, Y., Takakura, Y., Mitani, S., & Fujigaki, H. (2016). Depressive symptoms as a side effect of Interferon-alpha therapy induced by induction of indoleamine 2,3-dioxygenase 1. *Scientific Reports*, *6*, 29920.

Murray, C. J., & Lopez, A. D. (1996). Evidence-based health policy–lessons from the global burden of disease study. *Science*, *274*, 740–743.

O'Connor, J. C., Lawson, M. A., Andre, C., Briley, E. M., Szegedi, S. S., Lestage, J., Castanon, N., Herkenham, M., Dantzer, R., & Kelley, K. W. (2009). Induction of IDO by bacille Calmette-Guerin is responsible for development of murine depressive-like behavior. *The Journal of Immunology*, *182*, 3202–3212.

O'Connor, J. C., Lawson, M. A., Andre, C., Moreau, M., Lestage, J., Castanon, N., Kelley, K. W., & Dantzer, R. (2009). Lipopolysaccharide-induced depressive-like behavior is mediated by indoleamine 2,3-dioxygenase activation in mice. *Molecular Psychiatry*, *14*, 511–522.

O'Connor, R. M., Dinan, T. G., & Cryan, J. F. (2012). Little things on which happiness depends: microRNAs as novel therapeutic targets for the treatment of anxiety and depression. *Molecular Psychiatry*, *17*, 359–376.

Otte, C., Gold, S. M., Penninx, B. W., Pariante, C. M., Etkin, A., Fava, M., Mohr, D. C., & Schatzberg, A. F. (2016). Major depressive disorder. *Nature Reviews Disease Primers*, *2*, 16065.

Oxenkrug, G. (2013). Serotonin-kynurenine hypothesis of depression: historical overview and recent developments. *Current Drug Targets*, *14*, 514–521.

Paxinos, G., & Franklin, K. B. J. (2004). *The mouse brain in stereotaxic coordinates*. Elsevier Academic Press.

Rolls, A., Shechter, R., London, A., Ziv, Y., Ronen, A., Levy, R., & Schwartz, M. (2007). Toll-like receptors modulate adult hippocampal neurogenesis. *Nature Cell Biology*, *9*, 1081–1088.

Rupaimoole, R., & Slack, F. J. (2017). MicroRNA therapeutics: towards a new era for the management of cancer and other diseases. *Nature Reviews Drug Discovery*, *16*, 203–222.

Salazar, A., Gonzalez-Rivera, B. L., Redus, L., Parrott, J. M., & O'Connor, J. C. (2012). Indoleamine 2,3-dioxygenase mediates anhedonia and anxiety-like behaviors caused by peripheral lipopolysaccharide immune challenge. *Hormones and Behavior*, *62*, 202–209.

Savitz, J. (2017). Role of kynurenine metabolism pathway activation in major depressive disorders. *Current Topics in Behavioral Neurosciences*, *31*, 249–267.

Schratt, G. (2009). Fine-tuning neural gene expression with microRNAs. *Current Opinion in Neurobiology*, *19*, 213–219.

Setiawan, E., Wilson, A. A., Mizrahi, R., Rusjan, P. M., Miler, L., Rajkowska, G., Suridjan, I., Kennedy, J. L., Rekkas, P. V., Houle, S., & Meyer, J. H. (2015). Role of translocator protein density, a marker of neuroinflammation, in the brain during major depressive episodes. *JAMA Psychiatry*, *72*, 268–275.

Shelton, R. C., Claiborne, J., Sidoryk-Wegrzynowicz, M., Reddy, R., Aschner, M., Lewis, D. A., & Mirnics, K. (2011). Altered expression of genes involved in inflammation and apoptosis in frontal cortex in major depression. *Molecular Psychiatry*, *16*, 751–762.

Singhal, G., & Baune, B. T. (2017). Microglia: An interface between the loss of neuroplasticity and depression. *Frontiers in Cellular Neuroscience*, *11*, 270.

Smith, A. J., Smith, R. A., & Stone, T. W. (2009). 5-Hydroxyanthranilic acid, a tryptophan metabolite, generates oxidative stress and neuronal death via p38 activation in cultured cerebellar granule neurones. *Neurotoxicity Research*, *15*, 303–310.

Stone, T. W., & Darlington, L. G. (2002). Endogenous kynurenines as targets for drug discovery and development. *Nature Reviews Drug Discovery*, *1*, 609–620.

Tang, C. Z., Zhang, D. F., Yang, J. T., Liu, Q. H., Wang, Y. R., & Wang, W. S. (2019). Overexpression of microRNA-301b accelerates hippocampal microglia activation and cognitive impairment in mice with depressive-like behavior through the NF-kappaB signaling pathway. *Cell Death & Disease*, *10*, 316.

Tashiro, T., Murakami, Y., Mouri, A., Imamura, Y., Nabeshima, T., Yamamoto, Y., & Saito, K. (2017). Kynurenine 3-monooxygenase is implicated in antidepressants-responsive depressive-like behaviors and monoaminergic dysfunctions. *Behavioral Brain Research*, *317*, 279–285.

Treadway, M. T., Waskom, M. L., Dillon, D. G., Holmes, A. J., Park, M. T. M., Chakravarty, M. M., Dutra, S. J., Polli, F. E., Iosifescu, D. V., Fava, M., Gabrieli, J. D. E., & Pizzagalli, D. A. (2015). Illness progression, recent stress, and morphometry of hippocampal subfields and medial prefrontal cortex in major depression. *Biological Psychiatry*, *77*, 285–294.

Walter, S., Letiembre, M., Liu, Y., Heine, H., Penke, B., Hao, W., Bode, B., Manietta, N., Walter, J., Schulz-Schüffer, W., & Fassbender, K. (2007). Role of the toll-like receptor 4 in neuroinflammation in Alzheimer's disease. *Cellular Physiology and Biochemistry*, *20*, 947–956.

Wulaer, B., Kunisawa, K., Hada, K., Jaya Suento, W., Kubota, H., Iida, T., Kosuge, A., Nagai, T., Yamada, K., Nitta, A., Yamamoto, Y., Saito, K., Mouri, A., & Nabeshima, T. (2020). Shati/Nat8l deficiency disrupts adult neurogenesis and causes attentional impairment through dopaminergic neuronal dysfunction in the dentate gyrus. *Journal of Neurochemistry*, https://doi.org/10.1111/jnc.15022

Yamada, K., Iida, R., Miyamoto, Y., Saito, K., Sekikawa, K., Seishima, M., & Nabeshima, T. (2000). Neurobehavioral alterations in mice with a targeted deletion of the tumor necrosis factor-alpha gene: implications for emotional behavior. *Journal of Neuroimmunology*, *111*, 131–138.

Yamawaki, Y., Yoshioka, N., Nozaki, K., Nozaki, K., Ito, H., Oda, K., Harada, K., Shirawachi, S., Asano, S., Aizawa, H., Yamawaki, S., Kanematsu, T., & Akagi, H. (2018). Sodium butyrate abolishes lipopolysaccharide-induced depression-like behaviors and hippocampal microglial activation in mice. *Brain Research*, *1680*, 13–38.

Zou, W., Feng, R., & Yang, Y. (2018). Changes in the serum levels of inflammatory cytokines in antidepressant drug-naive patients with major depression. *PLoS One*, *13*, e0197267.

SUPPORTING INFORMATION

Additional supporting information may be found online in the Supporting Information section.

How to cite this article: Suento WJ, Kunisawa K, Wulaer B, et al. Prefrontal cortex miR-874-3p prevents lipopolysaccharide-induced depression-like behavior through inhibition of indoleamine 2,3-dioxygenase 1 expression in mice. *J Neurochem*. 2020;00:1–16. https://doi.org/10.1111/jnc.15222

Prefrontal cortex miR-874-3p prevents lipopolysaccharide-induced depression-like behavior through inhibition of indoleamine 2,3-dioxygenase 1 expression in mice

ORIGINALITY REPORT

25%	%3	41%	5%
SIMILARITY INDEX	INTERNET SOURCES	PUBLICATIONS	STUDENT PAPERS

PRIMARY SOURCES

1	ir.soken.ac.jp Internet Source	2%
2	www.jstage.jst.go.jp Internet Source	2%
3	pericles.pericles-prod.literatumonline.com Internet Source	2%
4	Jureepon Roboon, Tsuyoshi Hattori, Hiroshi Ishii, Mika Takarada - Iemata et al. " Inhibition of CD38 and supplementation of nicotinamide riboside ameliorate lipopolysaccharide - induced microglial and astrocytic neuroinflammation by increasing NAD ", Journal of Neurochemistry, 2021 Publication	2%
5	www.biorxiv.org Internet Source	2%
6	Yuko Mori, Akihiro Mouri, Kazuo Kunisawa, Mami Hirakawa et al. "Kynurenine 3-	2%

monooxygenase deficiency induces depression-like behavior via enhanced antagonism of α7 nicotinic acetylcholine receptors by kynurenic acid", Behavioural Brain Research, 2021
Publication

---

7 Tomoyuki Tashiro, Yuki Murakami, Akihiro Mouri, Yukio Imamura, Toshitaka Nabeshima, Yasuko Yamamoto, Kuniaki Saito. "Kynurenine 3-monooxygenase is implicated in antidepressants-responsive depressive-like behaviors and monoaminergic dysfunctions", Behavioural Brain Research, 2017 — 1 %
Publication

---

8 Kazuo Kunisawa, Takeshi Shimizu, Itaru Kushima, Branko Aleksic et al. "Dysregulation of schizophrenia-related aquaporin 3 through disruption of paranode influences neuronal viability", Journal of Neurochemistry, 2018 — 1 %
Publication

---

9 www.scopus.com — 1 %
Internet Source

---

10 www.jneurosci.org — 1 %
Internet Source

---

11 Anthony Laugeray, Jean-Marie Launay, Jacques Callebert, Oguz Mutlu, Gilles J. Guillemin, Catherine Belzung, Pascal R. Barone. "Chronic Treatment with the IDO1 — 1 %

Inhibitor 1-Methyl-D-Tryptophan Minimizes the Behavioural and Biochemical Abnormalities Induced by Unpredictable Chronic Mild Stress in Mice - Comparison with Fluoxetine", PLOS ONE, 2016
Publication

---

12 Yuki Murakami, Yukio Imamura, Yoshiyuki Kasahara, Chihiro Yoshida et al. "The Effects of Maternal Interleukin-17A on Social Behavior, Cognitive Function, and Depression-Like Behavior in Mice with Altered Kynurenine Metabolites", International Journal of Tryptophan Research, 2021 — 1 %
Publication

---

13 www.mdpi.com — 1 %
Internet Source

---

14 Bolati Wulaer, Kazuhiro Hada, Akira Sobue, Norimichi Itoh, Toshitaka Nabeshima, Taku Nagai, kiyofumi yamada. "Overexpression of Astroglial Major Histocompatibility Complex Class I in the Medial Prefrontal Cortex Impairs Visual Discrimination Learning in Mice", Research Square, 2020 — 1 %
Publication

---

15 scholarworks.iupui.edu — 1 %
Internet Source

---

16 academic.oup.com — 1 %
Internet Source

17	hdl.handle.net Internet Source	1 %
18	Geoffroy Laumet, Jules Daniel Edralin, Angie Chi-An Chiang, Robert Dantzer, Cobi J. Heijnen, Annemieke Kavelaars. "Resolution of inflammation-induced depression requires T lymphocytes and endogenous brain interleukin-10 signaling", Neuropsychopharmacology, 2018 Publication	1 %
19	Akihiro Mouri, Yuta Hoshino, Shiho Narusawa, Keisuke Ikegami et al. "Thyrotoropin receptor knockout changes monoaminergic neuronal system and produces methylphenidate-sensitive emotional and cognitive dysfunction", Psychoneuroendocrinology, 2014 Publication	1 %
20	Hisako Kubo, Masato Hoshi, Akihiro Mouri, Chieko Tashita, Yasuko Yamamoto, Toshitaka Nabeshima, Kuniaki Saito. "Absence of kynurenine 3-monooxygenase reduces mortality of acute viral myocarditis in mice", Immunology Letters, 2017 Publication	1 %
21	Ling Mei, Min Li, Tao Zhang. "MicroRNA miR-874-3p inhibits osteoporosis by targeting leptin (LEP)", Bioengineered, 2021	1 %

Publication

22	www.spandidos-publications.com Internet Source	1 %
23	Submitted to Georgia Institute of Technology Main Campus Student Paper	<1 %
24	Xin-Ya Qin, Qing-Hong Shan, Hui Fang, Yu Wang, Peng Chen, Zhi-Qi Xiong, Dick F. Swaab, Jiang-Ning Zhou. "PSD-93 up-regulates the synaptic activity of corticotropin-releasing hormone neurons in the paraventricular nucleus in depression", Acta Neuropathologica, 2021 Publication	<1 %
25	www.nature.com Internet Source	<1 %
26	Sun-fu Zhang, Jun-chen Chen, Jing Zhang, Jian-guo Xu. "miR-181a involves in the hippocampus-dependent memory formation via targeting PRKAA1", Scientific Reports, 2017 Publication	<1 %
27	www.tandfonline.com Internet Source	<1 %
28	Marcus A Lawson, Jennifer M Parrott, Robert H McCusker, Robert Dantzer, Keith W Kelley, Jason C O'Connor. "Intracerebroventricular administration of lipopolysaccharide induces	<1 %

indoleamine-2,3-dioxygenase-dependent depression-like behaviors", Journal of Neuroinflammation, 2013
Publication

29	journals.plos.org Internet Source	<1 %
30	Akira Sobue, Norimichi Ito, Taku Nagai, Wei Shan et al. "Astroglial major histocompatibility complex class I following immune activation leads to behavioral and neuropathological changes", Glia, 2018 Publication	<1 %
31	researchmap.jp Internet Source	<1 %
32	Akihiro Mouri, Mayu Ukai, Mizuki Uchida, Sho Hasegawa et al. "Juvenile social defeat stress exposure persistently impairs social behaviors and neurogenesis", Neuropharmacology, 2018 Publication	<1 %
33	Kazuo Kunisawa, Willy Jaya Suento, Bolati Wulaer, Aika Kosuge et al. "前頭前皮質のmiR-874-3pはIDO1抑制を介してLPS誘発性のうつ様行動を緩解する", Proceedings for Annual Meeting of The Japanese Pharmacological Society, 2021 Publication	<1 %

34	Submitted to University of Oklahoma Student Paper	<1%
35	Xiuqing Zhu, Jinqing Hu, Shuhua Deng, Yaqian Tan et al. "Comprehensive Bibliometric Analysis of the Kynurenine Pathway in Mood Disorders: Focus on Gut Microbiota Research", Frontiers in Pharmacology, 2021 Publication	<1%
36	scholars.uthscsa.edu Internet Source	<1%
37	Kazuo Kunisawa, Kiwamu Kido, Natsuki Nakashima, Takuya Matsukura, Toshitaka Nabeshima, Masayuki Hiramatsu. "Betaine attenuates memory impairment after water-immersion restraint stress and is regulated by the GABAergic neuronal system in the hippocampus", European Journal of Pharmacology, 2017 Publication	<1%
38	Le Wang, Xiaoli Gong, Yang Liu, Tianshu Du, Zhen Zhang, Ting Zhang, Xiaomin Wang. "CD200 maintains the region - specific phenotype of microglia in the midbrain and its role in Parkinson's disease", Glia, 2020 Publication	<1%
39	tel.archives-ouvertes.fr Internet Source	<1%